Supplemental data

1. Visual assessment of spheroid circularity and compactness

To assess the circularity and compactness of the spheroids, blinded observers were asked to score each category, out of a 5-point scale, by comparing images of spheroids to the following visual guide. In each category, the lack of a visible spheroid or formation of multiple spheroids receives a score of 1. For compactness, the primary metric on which spheroids were evaluated is intercellular spacing. Spheroid with clearly visible spaces and gaps were classified as a loose aggregate (score = 2), and aggregates with no gaps within the cell mass but presenting diffuse boarders were scored as a tight aggregate (score = 3). Further compaction lead to the formation of distinct dark boarders around spheroids with few loose cells attached, these were classified as compact spheroid (score = 4). At the most compact stage cells on the surface of the spheroid were remodeled and follow the contour of the spheroid, creating a smooth and defined outline and were classified as tight spheroids (score = 5)

For circularity, spheroids that possessed similar degrees of concave and convex outline were classified as irregular (score = 2), whereas those that consist mostly of convex borders but with small concave dimples were classified as minor irregular (score =3). Spheroids that are elongated with no concave outline sections receive a score of 4, and finally, symmetrically circular spheroids receive a score of 5.

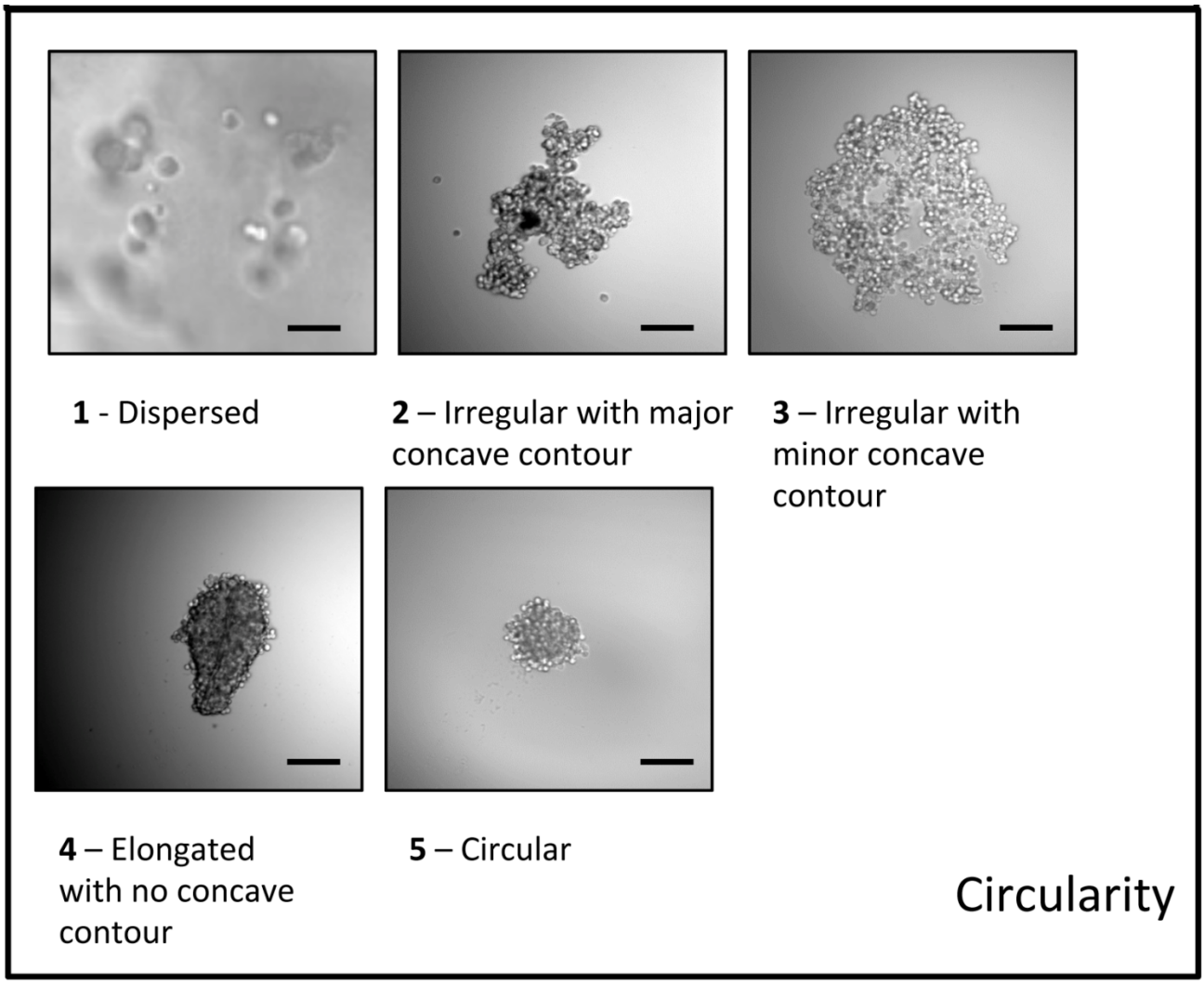

Figure S1: Scoring guide given to blinded scorer for the assignment of circularity score.

Scale bar = 200 μm

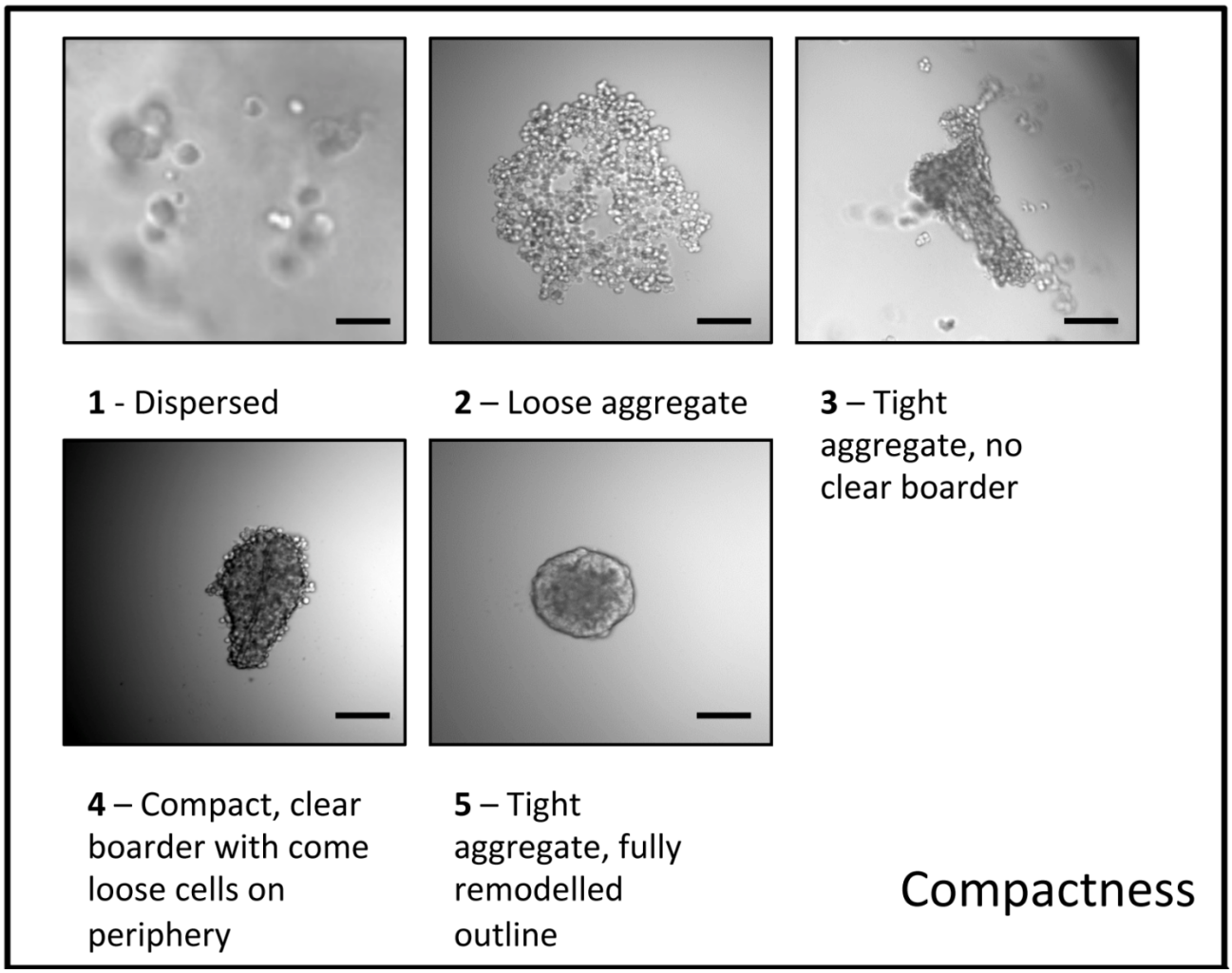

Figure S2: Scoring guide given to blinded scorer for the assignment of compactness score. Scale bar = 200 μm

2. Assessment of spheroid circularity using image analysis algorithm

A commonly adopted method to characterize spheroid morphology is by automated images analysis algorithm. Generally the method begins by creating a binary image from the original grayscale file, followed by automated edge detection and measurement of enclosed area. Using the same open source software and edge detection algorithm for motion tracking, we have generated outline traces for each of the image files used for visual grading. Images that lack of a visible spheroid or contain multiple spheroids were not scored. The outline traces were analyzed using ImageJ (NIH, MD http://imagej.nih.gov/ij/) to generate circularity measurements. Circularity is defined as followed.

$$Circularity = 4\pi \times \frac{[area]}{[perimeter]^2}$$

Circularity value of 1 (maximum) indicates that the spheroid is perfectly circular. A decreasing value towards 0 indicated the spheroid is more elongated and less circular. This protocol does not require user intervention and therefore is compatible with automated high throughput screen platforms. Comparison between the two methods is shown in Figure S3A. Standard deviations of circularity values measured by image-based analysis is shown in Figure S3B.

In general, the two quantification methods generate similar conclusions regarding the effects of additives on spheroid circularity. In MethCel only samples, the presence of additive improves spheroid circularity for all cell types in a dose dependent manner, with the exception of PC3and HEK 293. For spheroid cultured with collagen and MethoCel, the 5-point visual scale tends to yield a higher circularity score compared to image

analysis protocol. This difference in most pronounced at high collagen concentration (141 μg/mL), where the image based edge detection often fail to generate a consistent outline due to adhesion of spheroid to the hanging drop and the presence of uneven background lighting. In contrast, the 5-point visual scale is relatively immune to these artifacts since human can easily decipher edge of spheroid from background.

We noted some discrepancies in circularity values between those scored by human observers versus automated image analysis, even though the tends in circularity change due to the presence of additives are similar between the two scoring method. One reason that the absolute values of circularity may appear to be different is because the image-based algorithms used area and perimeter values to calculate circularity. In cases where the boarder of a spheroid appears rough, the software may generate excessively contoured outline thus increasing the perimeter value, leading to a low circularity measure. In contrast, a human observer will be less sensitive of these small variations in roughness on the spheroid and focus more on the overall roundness, thus yielding a differ (and often higher) circularity value. Also, the visual scale consist of much larger grading scale (min=0.5) and contain less intervals compared to the continuous circularity values given by image-based analysis and therefore can be more prone to systemic over- or under-estimation.

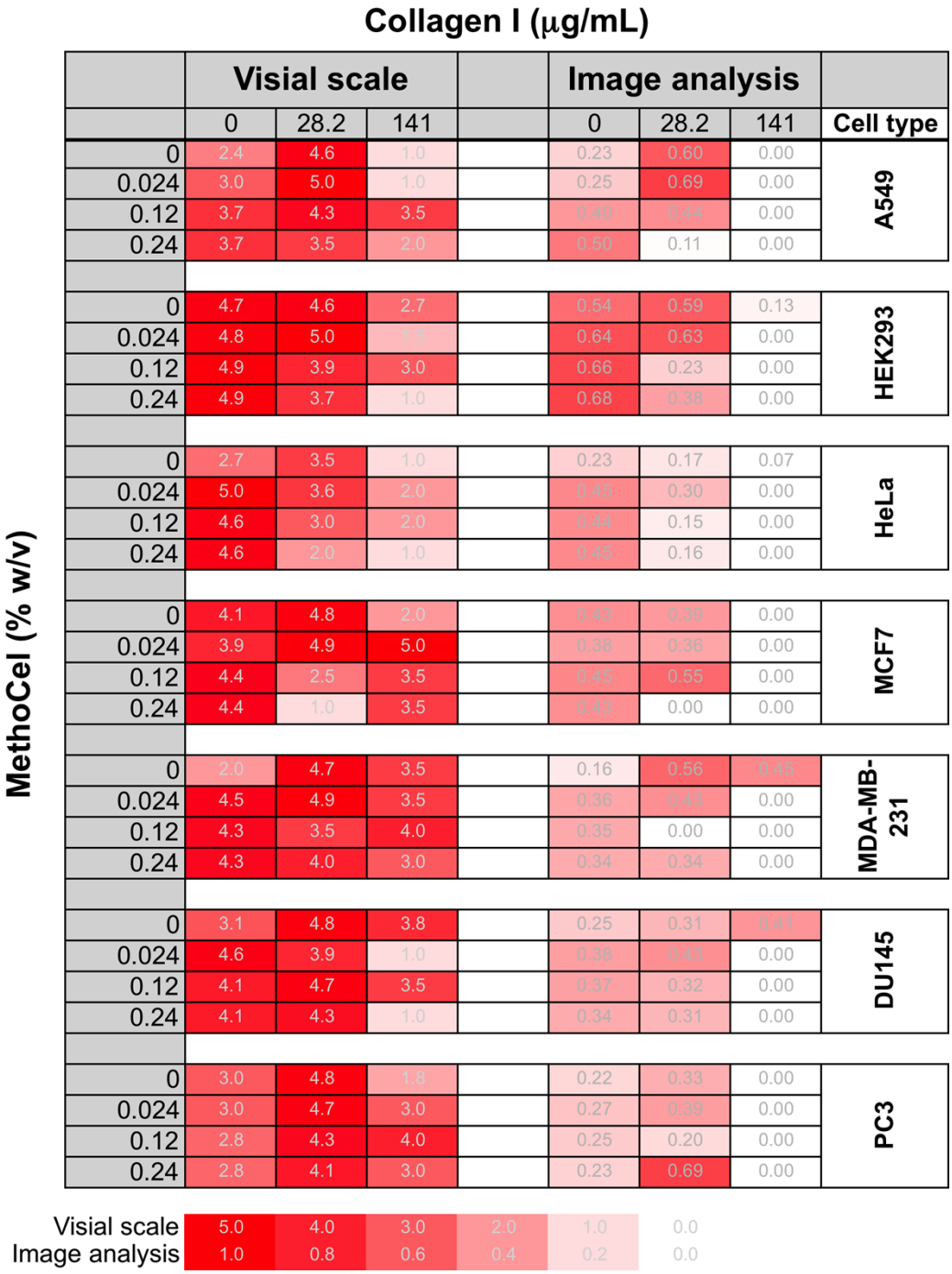

Figure S3A: Comparison of circularity measurements using 5-point visual scale (section S1) versus automated image analysis (section S2).

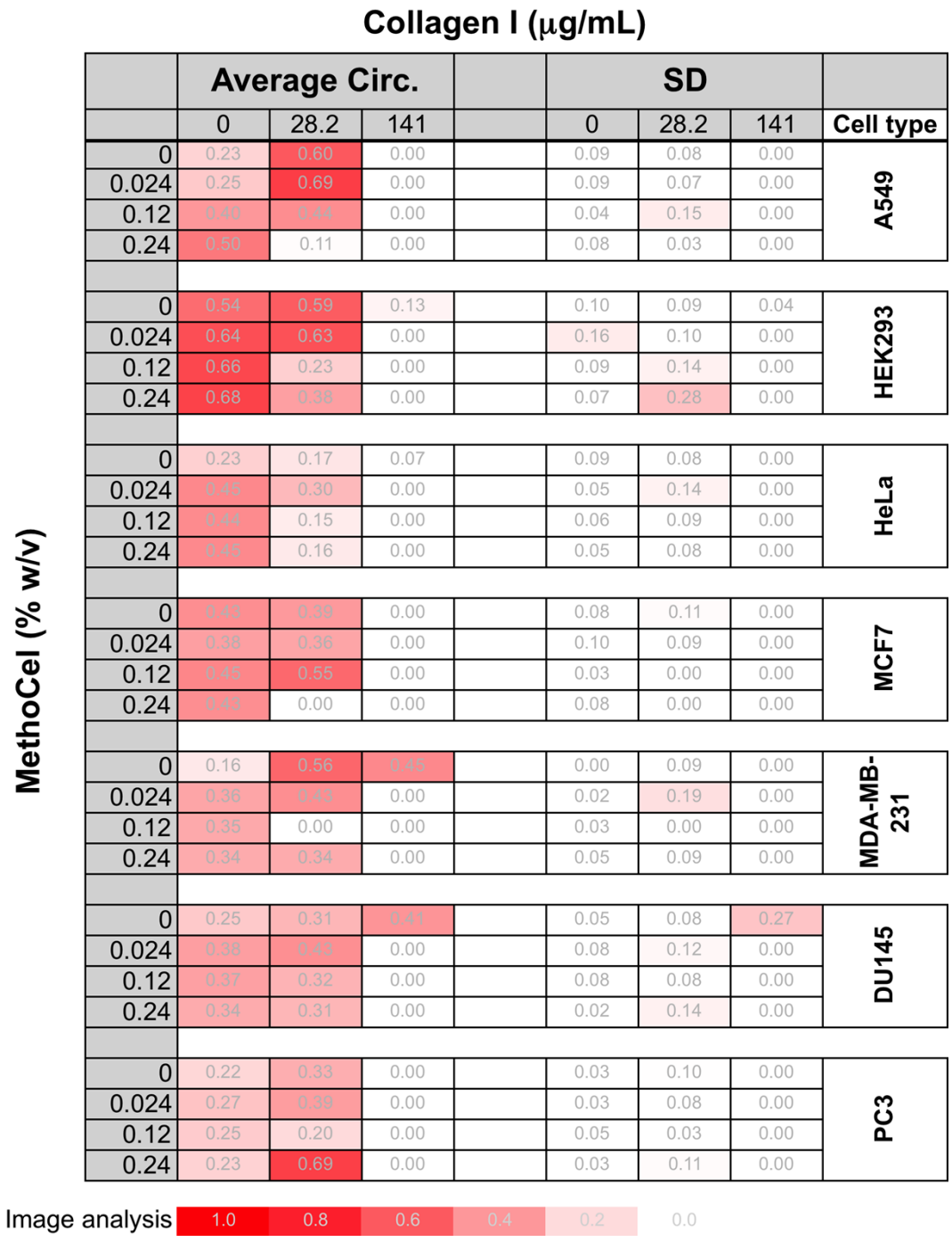

Figure S3B: Average circularity values with standard deviations (N=5) of spheroid as measured using automated image analysis algorithm (section S2). Standard deviations are generally small

and tend to increase at high collagen concentration where imaging artifacts and other interference become prevent.

3. Long term stability and consistency of spheroid formation using hanging drop plate

High Throughput Hanging Drop Array Plates were initially developed(1), and then further refined for long term stable culturing in the micro droplet format(2). The optimized plate design was used due to their well-established, robust hanging drop cultures allowing for long term, consistent culturing. These design considerations resulted in uniform droplet generation across the entire plate with excellent Z-factor(3) with small inter-droplet variability. In practice this translates to very uniform spheroid morphology within the same cell type and cell number, thus a small number of spheroid are needed to demonstrate difference between different conditions. This is supported by the small standard deviation in circularity score measured by image analysis algorithm (Figure S3B). Additionally due to the microdroplet geometric reproducibility, and maintained droplet structure, cells experience similar culturing conditions regardless the droplet, unlike more typical hanging drops on flat substrates (i.e. tissue culture plate lids).

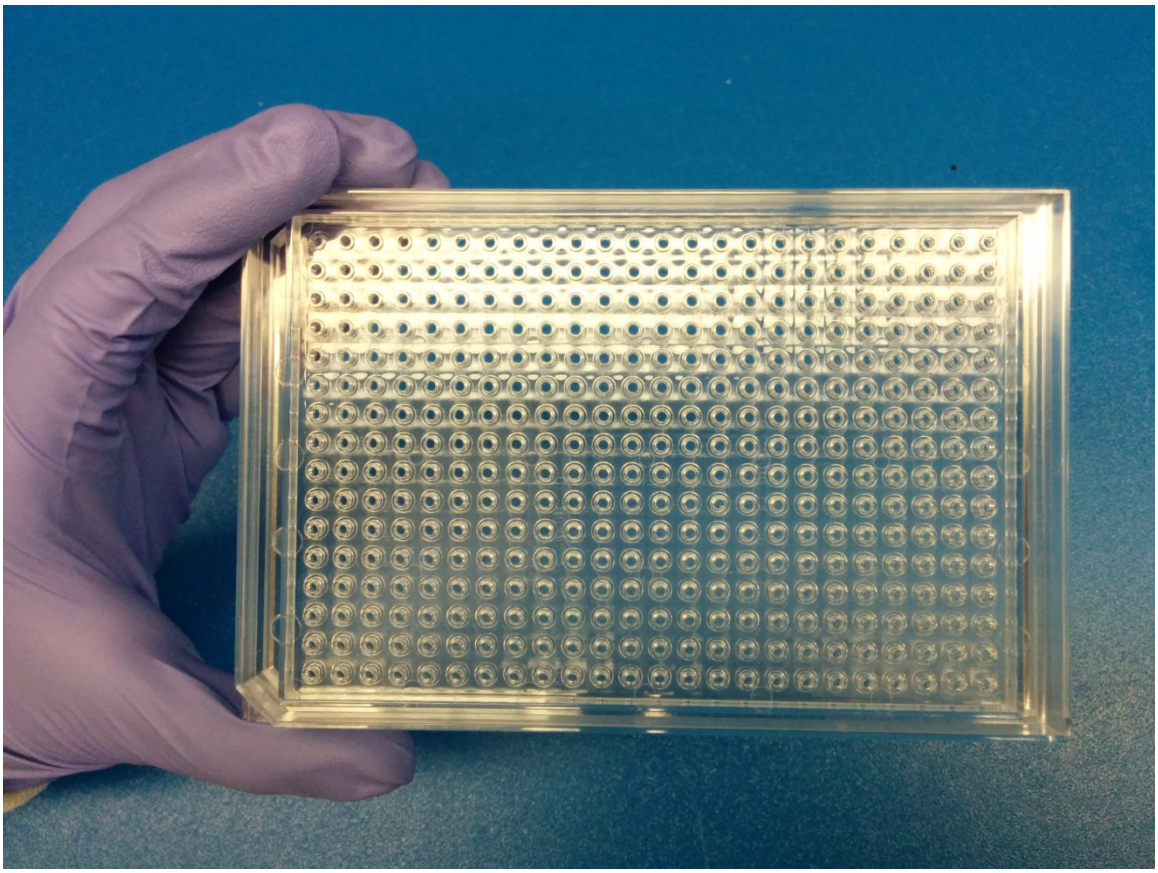

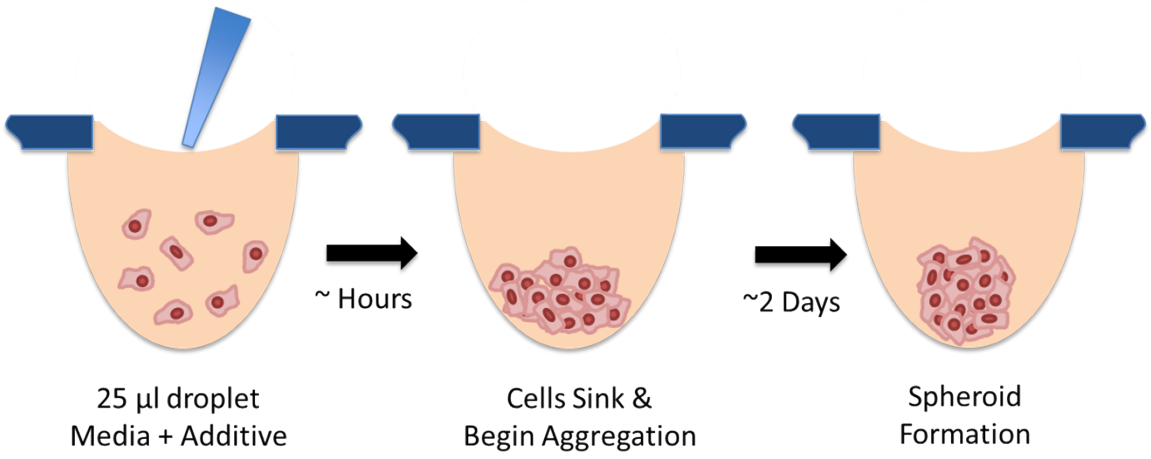

Figure S4: (Top) 384 hanging drop spheroid culture array plate. (Bottom) Illustration of hanging drop formation to produce spheroids. Briefly, the pipette is inserted into the access hole, where the cells and media are pipetted out, delivering the sample into the hanging drop plate. The hydrophilic plate surface results in the formation of a droplet confined by the geometry of the plate. Within a few hours, cells will sink to the bottom of the hanging

drop and begin aggregating, if possible. Approximately two days later, spheroids will form, assuming the cells are capable of generating spheroids.

References

1. Tung Y.C., Hsiao A.Y., Allen S.G., Torisawa Y.S., Ho M. and Takayama S. High-throughput 3D spheroid culture and drug testing using a 384 hanging drop array. The Analyst 136(3):473-478, 2011.
2. Hsiao A.Y., Tung Y.C., Kuo C.H., Mosadegh B., Bedenis R., Pienta K.J. and Takayama S. Micro-ring structures stabilize microdroplets to enable long term spheroid culture in 384 hanging drop array plates. Biomed Microdevices 14(2):313-323, 2012.
3. Hsiao A.Y., Tung Y.C., Qu X., Patel L.R., Pienta K.J. and Takayama S. 384 hanging drop arrays give excellent Z-factors and allow versatile formation of co-culture spheroids. Biotechnol Bioeng 109(5):1293-1304, 2012.